

## EVALUATING REPETITION IN SEDIMENTARY SUCCESSIONS USING HIGH RESOLUTION INTEGRATED STRATIGRAPHY: AN EXAMPLE IN THE LOWER PLIOCENE SEQUENCE OF ODP HOLE 975B

AGATA DI STEFANO

Received: October 27, 2009; accepted: February 2, 2010

**Key words:** Balearic Basin, Early Pliocene, calcareous nannofossil biostratigraphy, cyclostratigraphy, repeated stratigraphy.

**Abstract.** The Lower Pliocene succession recovered at ODP Hole 975B (Balearic Basin, western Mediterranean) displays a sudden increase in sedimentation rate, in disagreement with the lithological homogeneity that characterizes the succession. The present study, consisting of a high resolution stratigraphic analysis, demonstrates that the succession is affected by repetition. The section has been astrochronologically constrained through integration of detailed biostratigraphy and cyclostratigraphy, which permitted a precise evaluation of the length and duration of the duplicated interval. This result demonstrates the efficacy of integrated stratigraphy in solving wide-range geological problems.

**Riassunto.** Il Site ODP 975 è ubicato in Mediterraneo occidentale tra l'Arcipelago Balearico e il Bacino Algerino. Si tratta di una successione prevalentemente costituita da *ooze* carbonatici di età compresa tra il Pleistocene e il Miocene sommitale. Il limite Miocene/Pliocene, riconosciuto alla profondità di 305.22 m, è marcato da un brusco cambio litologico tra micriti sabbiose finemente laminate, di età messiniana, e fanghi pelagici a foraminiferi e nannofossili calcarei di età zancleana.

Dati di letteratura indicano per l'intervallo del Pliocene Inferiore (tra il limite Miocene/Pliocene e il top della carota 27 a 244.80 m) tassi di sedimentazione molto differenti, con un brusco passaggio da valori medi di circa 40 m/Ma a circa 70m/Ma. Questi valori contrastano fortemente con l'evidenza di un'omogeneità litologica, che lascerebbe presupporre tassi di sedimentazione relativamente costanti.

L'analisi biostratigrafica quantitativa ad alta risoluzione dei nannofossili calcarei, unita a uno studio ciclostratigrafico basato sulle variazioni del contenuto di CaCO<sub>3</sub>, dimostra che il brusco cambio nel tasso di sedimentazione nella successione in oggetto, finora ritenuta continua e indisturbata, è legato alla presenza di una ripetizione stratigrafica. Il tratto di sezione ripetuta è di 19.40 m (tra 298.4-279.0 e 279.0-259.6 mbsf) e corrisponde a un intervallo di tempo di circa 0.563 My.

Pertanto, in questo studio viene messa in evidenza l'efficacia dell'utilizzo della stratigrafia integrata ad alta risoluzione nella soluzione di problemi geologici anche ad ampia scala.

### Introduction

ODP Hole 975B is drilled at 2415 m water depth in the western Mediterranean on the South Balearic Margin between the Balearic Promontory (Menorca and Mallorca Islands) and the Algerian Basin (38°53.786'N, 4°30.596'E) (Fig. 1). The recovered suc-

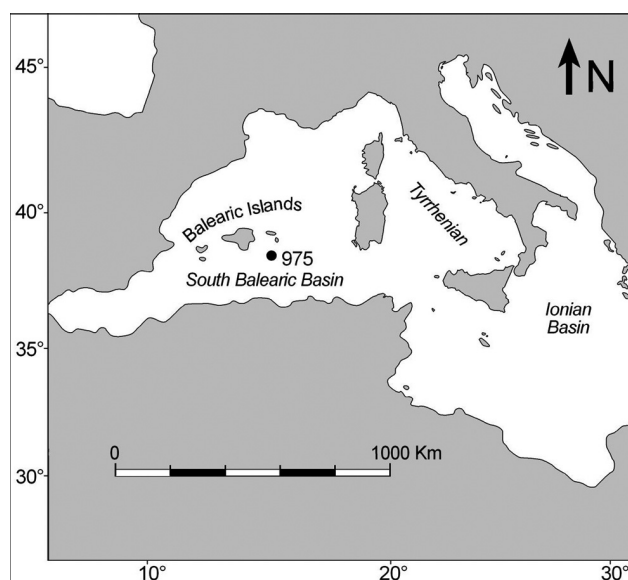


Fig. 1 - Location map of ODP Site 975 (38°53.786'N, 4°30.596'E), Western Mediterranean, south of Balearic Arcipelago (2415 m water depth).

cession mainly consists of nannofossil or calcareous clays of Pliocene to Pleistocene age, characterized by cyclic alternations of lighter and darker intervals. The Miocene/Pliocene boundary (M/Pb) was recorded at

305.22 mbsf and is marked by a sharp lithological change (Comas et al. 1996).

In the lithostratigraphic interval spanning from the M/Pb and the top of core 27 (244.80 mbsf) a set of planktonic foraminifer biostratigraphic events (Iaccarino et al. 1999a, b; Serrano et al. 1999) have been determined. Their positions along the section is shown in Fig. 2. According to these biostratigraphic data, the Lower Pliocene biozones from MPI1 to MPI3 (Cita 1975; Sprovieri 1993) were recognized. The age-depth diagram (Fig. 3) obtained through plotting the ages of the considered biohorizons in relation to their position along the section, clearly indicates that in the lowermost part the average sedimentation rate is of about 40 m/My, whilst in the upper part the rates are up to about 70 m/My (Comas et al. 1996, fig. 34).

This sudden and abrupt change in accumulation rate is unexpected and difficult to explain in the absence of any marked lithological and sedimentological changes. No explanation was previously given to the change in sedimentation rate recorded in the ODP Site 975 succession, which is described as a continuous and almost undisturbed sedimentary sequence for the Pliocene-Pleistocene interval on the Menorca Rise (Comas et al. 1996).

The aim of the present study is to understand the anomalous increase of sedimentation rate associated with a lack of lithological and sedimentological variations and to establish the effective continuity of the section, excluding disturbed parts.

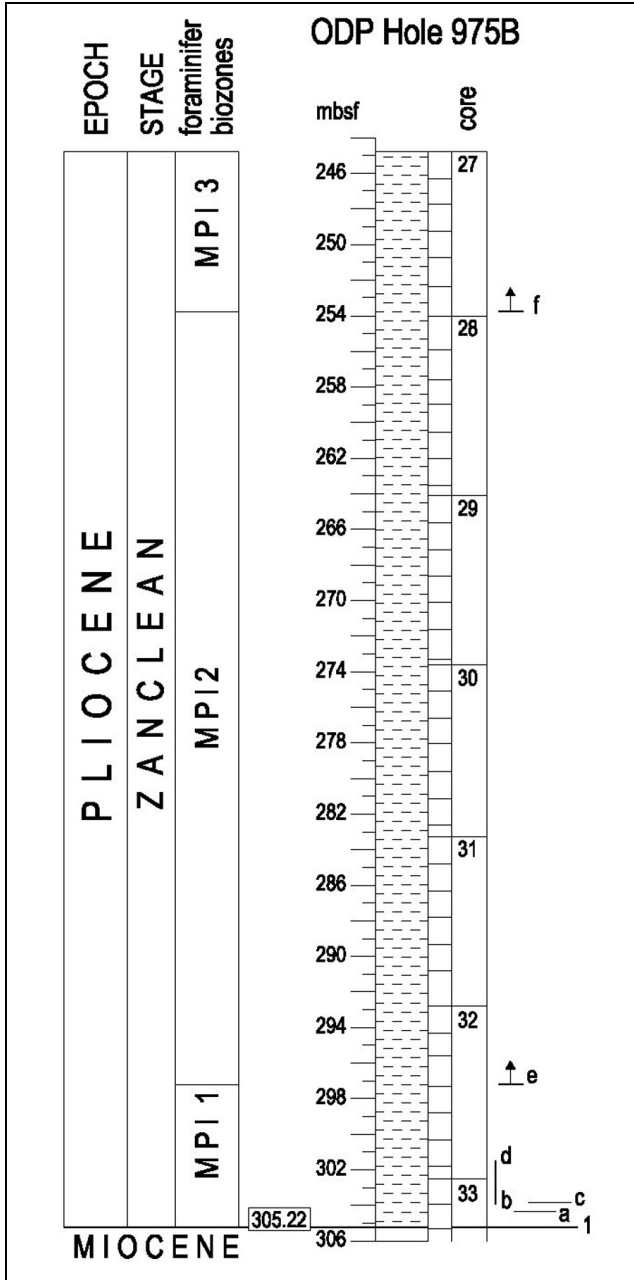


Fig. 2 - Stratigraphic interval of the ODP Hole 975B succession from the Miocene/Pliocene boundary (1) between samples 33X-2, 139 cm and 33X-2, 125 cm (305.22 mbsf) to the top of core 27 at 244.80 mbsf. Positions of planktonic foraminifer events according to Iaccarino et al. (1999a; 1999b) and Serrano et al. (1999): a. First shift of dominantly sinistral *Neogloboquadrina acostanesis* (304.36 mbsf); b. Beginning of *Sphaeroidinellopsis* Acme (303.96 mbsf); c. First shift of dominantly sinistral *Neogloboquadrina acostanesis* (303,84 mbsf); d. End of *Sphaeroidinellopsis* Acme (301.50 mbsf); e. First Common Occurrence of *Globorotalia margaritae* (297.18 mbsf); f. First Occurrence of *Globorotalia puncticulata* (253.80 mbsf). Foraminifer biozones after Cita (1975) and Sprovieri (1993).

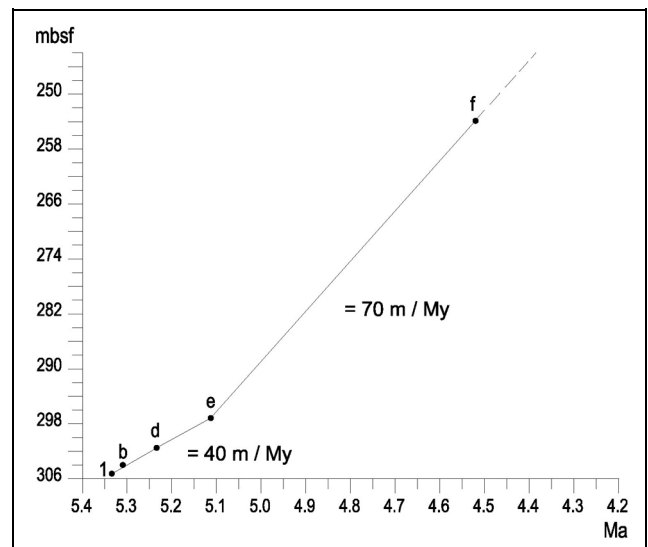


Fig. 3 - Age depth diagram and estimated sedimentation rates. Ages of bioevents after Sprovieri (1993) and Iaccarino et al. (1999a, b). 1. Miocene/Pliocene boundary (5.332 Ma, Lourens et al. 2004); b. Beginning (5.29 Ma) and d. End (5.20 Ma) of *Sphaeroidinellopsis* Acme; e. First Common Occurrence of *Globorotalia margaritae* (5.10 Ma); f. First Occurrence of *Globorotalia puncticulata* (4.52 Ma).

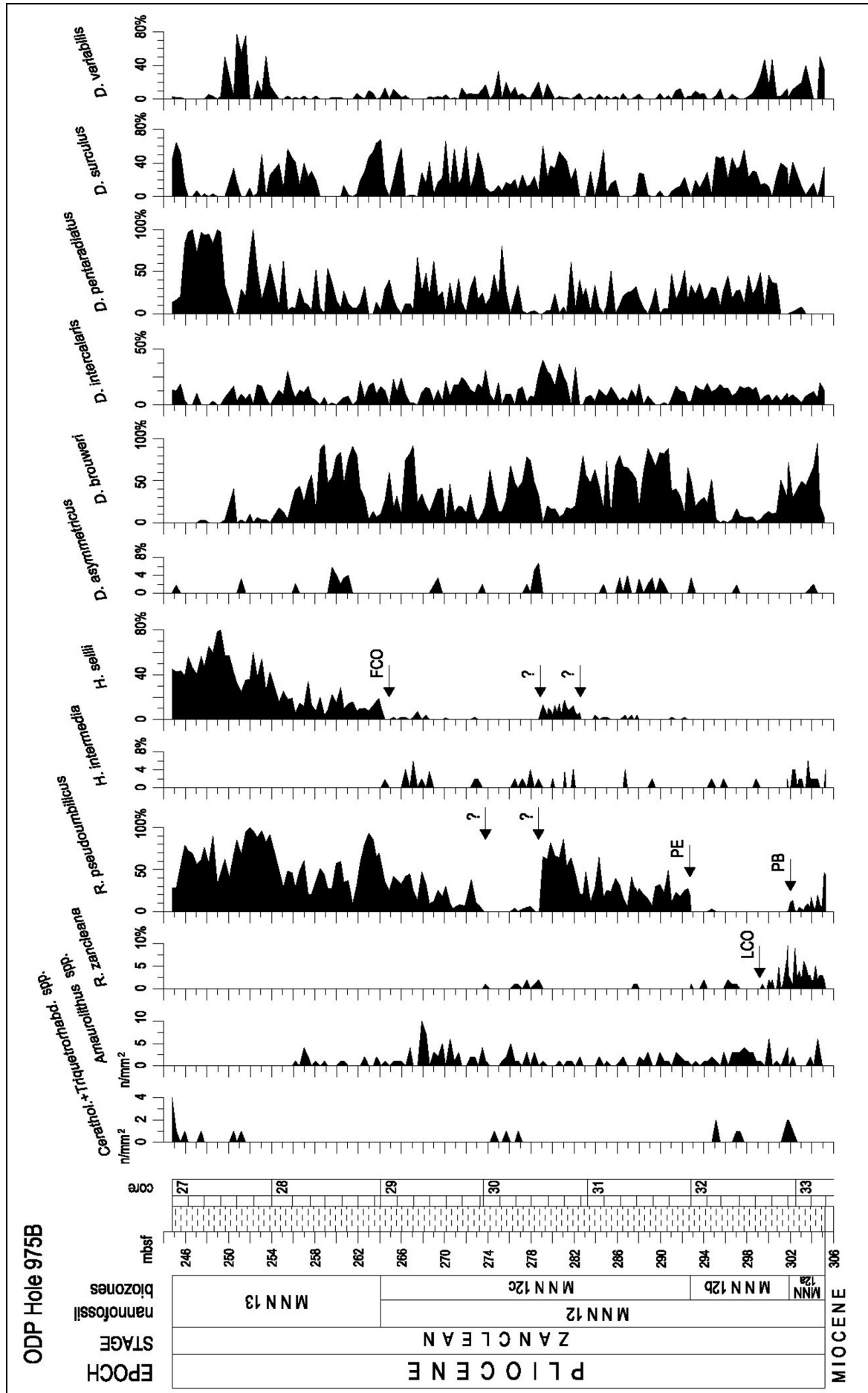


Fig. 4 - Quantitative distribution patterns of selected biostratigraphically useful nannofossil taxa, and positions of the most significant biohorizons. Nanofossil biozones after Rio et al. (1990) and Di Stefano & Sturiale (2010); LCO = Last Common Occurrence; FCO = First Common Occurrence; PB = Paracme Beginning; PE = Paracme End.

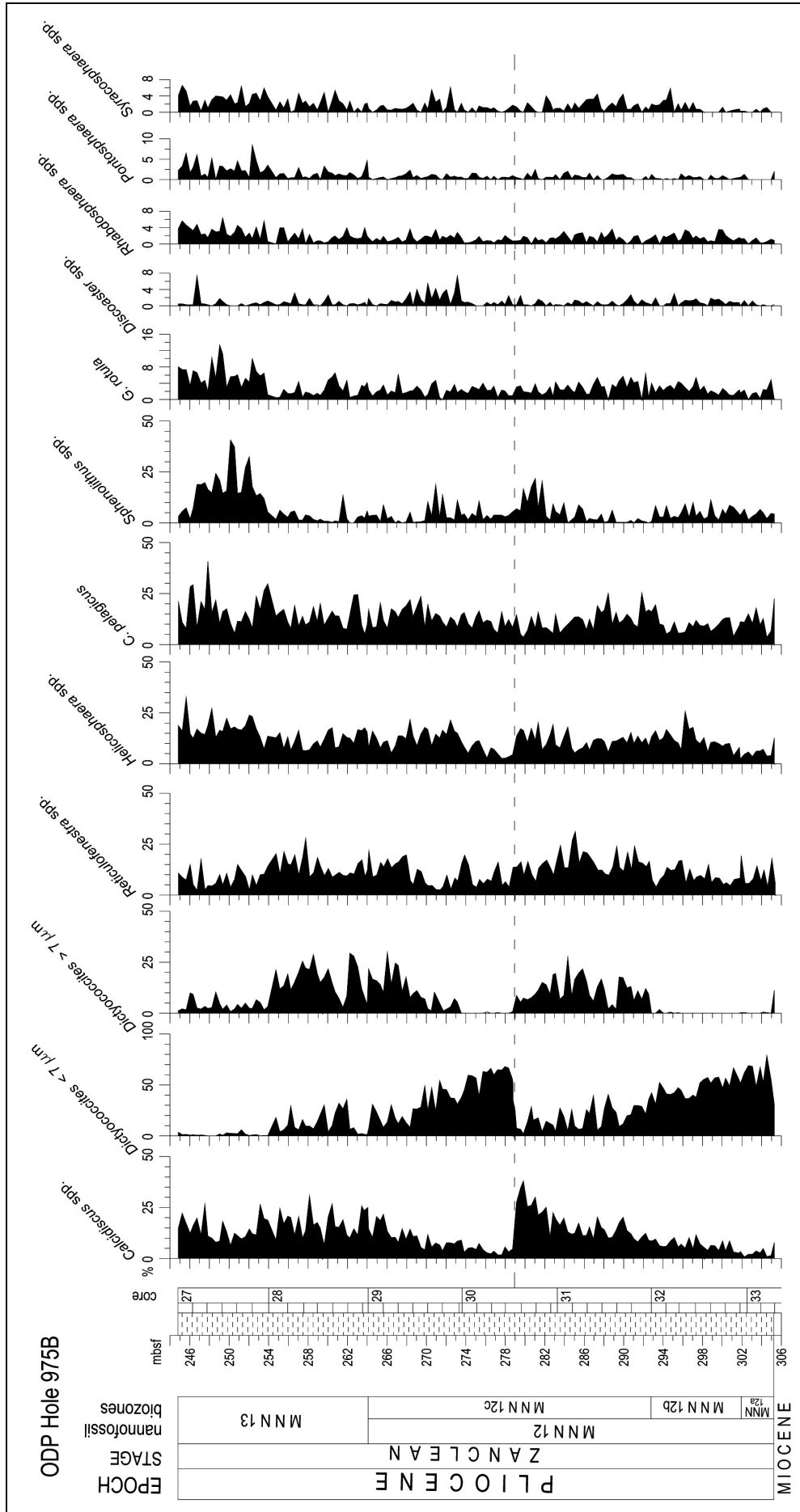


Fig. 5 - Quantitative distribution patterns of the main components of the nanofossil assemblages. Taxa that are present in percentages lower than 1% have not been considered. The dashed line indicates the point from which the supposed repetition of the section occurs, enhanced by a sudden change of the nanofossil assemblage composition.

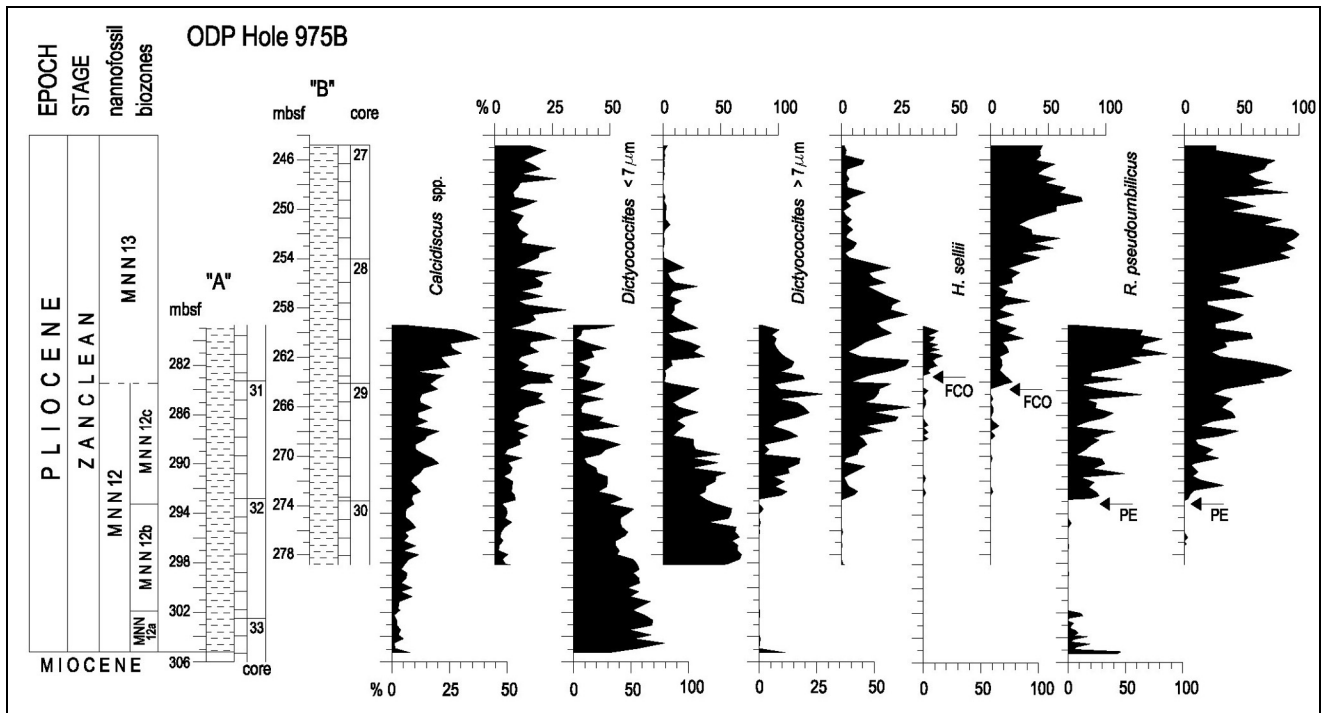


Fig. 6 - Partial overlap of two portions of the considered stratigraphic interval ("A" the lower and "B" the upper), according to the biostratigraphic evidence; several taxa show analogous trends within the overlapping intervals. Two different positions for both First Common Occurrence (FCO) of *Helicosphaera sellii* and Paracme End (PE) of *Reticulofenestra pseudoumbilicus* are recognized along the section.

ODP - Hole 975 B						
BIOEVENTS and ADDITIONAL "TIE-POINTS"	samples lower tract ("A")	mean depth "A" (mbsf)	samples upper tract ("B")	mean depth "B" (mbsf)	lithological cycles	Age (Ma) (Lourens et al.1996)
5	base cycle 55		27X-2.5cm - 27X-1.45 cm	246.30	55	4.082
4	base cycle 46		27X-6.25 cm - 27X-6.5 cm	252.45	46	4.288
i	FO <i>G. puncticulata</i>		28X-4.45 cm - 28X-4.25 cm	259.35	35	4.527
3	base cycle 34	30X-6.45 cm - 30X-6.25 cm	28X-5.105 cm - 28X-5.85 cm	261.45	34	4.552
h	FCO <i>H. sellii</i>	30X-7.5 cm - 30X-6.145 cm	29X-1.45 cm - 29X-1.5 cm	264.35	31	4.620
2	base cycle 22	31X-4.45 cm - 31X-4.25 cm	29X-4.65 cm - 29X-4.45 cm	269.15	22	4.835
g	PE <i>R. pseudoumbilicus</i>	32X-1.5 cm - 31X-7.45 cm	30X-1.25 cm - 30X-1.5 cm	273.75	14	5.004
f	FCO <i>G. margaritae</i>	32X-4.40 cm - 32X-3.116 cm			10	5.138
e	LCO <i>R. zancleana</i>	32X-5.65 cm - 32X-5.45 cm			7	5.199
d	AE <i>Sphaeroidinellopsis</i>	33X-6.144 cm - 33X-6.126 cm			6	5.234
c	2 <sup>nd</sup> sh <i>N. acostaensis</i> sx	33X-1.143 cm			2-3	5.310-5.290
b	AB <i>Sphaeroidinellopsis</i>	33X-2.10 cm - 33X-2.0 cm			2	5.310
a	1 <sup>st</sup> sh <i>N. acostaensis</i> sx	33X-2.50 cm - 33X-2.40 cm			1-2	5.332-5.310
1	Miocene/Pliocene boundary	33X-2.139 cm - 33X-2.125 cm			1	5.332

Tab. 1 - List of calcareous plankton bioevents considered in the present study (letters from "a" to "f") and other additional tie-points (numbers from "1" to "5"). Age of the Miocene/Pliocene boundary according to the ATNTS2004 (Lourens et al. 2004). The astrochronological inferred ages (Ma) to the bioevents refer to the lower boundary of the corresponding precessional cycles (according to Lourens et al. 1996). 1<sup>st</sup> sh = First Shift of sinistral (sx) coiling *N. acostaensis*; 2<sup>nd</sup> sh = Second Shift of sinistral (sx) coiling *N. acostaensis*; AB = Acme Beginning; AE = Acme End; LCO = Last Common Occurrence; FCO = First Common Occurrence; PE = Paracme End; FO = First Occurrence.

**Methods and Results**

The first step of the study consists of a detailed analysis of calcareous nanofossil contents, to improve the biostratigraphic resolution. Quantitative data have been collected with light microscope techniques (magnification of 1000x) on a total of 215 samples, taken at an average distance of 30 cm along the 65 m thick interval investigated. Smear slides have been prepared fol-

lowing standard methods (Fornaciari et al. 1996). Different counting methods were applied following Rio et al. (1990). Distribution patterns of species belonging to biostratigraphically significant genera are presented in Fig. 4. Percentages of *Discoaster* and *Helicosphaera* have been determined counting 50 specimens of each genus. *Reticulofenestra* frequencies have been calculated from counts of 100 specimens.

A revision of Lower Pliocene calcareous nannofossil biostratigraphy from the Mediterranean area (Sturiale 2008; Di Stefano & Sturiale 2010) has recently confirmed the rarity of the species traditionally used for identifying the M/Pb in open ocean areas: *Ceratolithus acutus* and *Triquetrorhabdulus rugosus*. These marker taxa are rare also at Hole 975B as shown by the observed total number of *Ceratolithus* spp. and *Triquetrorhabdulus* spp. (first graph in Fig. 4). These groups are determined scanning a minimum of 100 fields of view, and are reported as number of specimens/mm<sup>2</sup>.

In contrast to these poorly constrained marker taxa, the well-known paracme interval of *Reticulofenestra pseudoumbilicus* (Di Stefano et al. 1996, 1999; Sgarrella et al. 1999; Di Stefano & Sturiale 2010) and the range of the recently described *Reticulofenestra zancleana* (Di Stefano & Sturiale 2010) both show high biostratigraphical potential.

*Reticulofenestra zancleana* (Fig. 4) is present in the lower part of Hole 975B, with a maximum percentage of 12 % of the total *Reticulofenestra* population. Its Last Common Occurrence (LCO) is recorded at 299.35 mbsf. Specimens of *R. pseudoumbilicus* are present at the very base and become virtually absent just above, delineating a paracme interval from 301.95 to 292.75 mbsf. Unexpectedly, a second paracme interval is present from 279.0 to 273.45 mbsf.

*Helicosphaera sellii* is a marker species in the Early Pliocene (Rio et al. 1990; Di Stefano & Sturiale 2010). The First Common Occurrence (FCO) of the species seems to occur at the top of core 29 (264.35 mbsf), even if an “anomalous presence” of *H. sellii*, with frequencies up to 20%, is observable in the lower part of core 30, from 282.5 to 279.0 mbsf. *Helicosphaera intermedia* occurs discontinuously and in low frequencies in the lower 2/3 of the section.

Among discoasters, *D. pentaradiatus*, *D. surculus* and *D. brouweri* are the main species, all showing high variability in abundance. *Discoaster pentaradiatus* is dominant in the upper part, whilst *D. asymmetricus* is sporadically present. *Discoaster variabilis* is abundant in the lowermost part, scattered and less frequent in the central portion, and abundant again in a restricted interval at the top.

Abundance patterns within the total assemblage (Fig. 5), estimated by counting a minimum of 500 calcareous nannofossils larger than 3 µm, indicate that the main component is represented by “small” *Dictyococcites* spp. (3-7 µm), with maximum frequencies of 80%. Nevertheless, the decreasing trend shown by this group seems to be interrupted at about 279 mbsf (between samples 30X-4, 85 cm, 278.95 mbsf and 30X-4, 105 cm, 279.15 mbsf), where the frequency suddenly jumps up; from this point up, the group shows a decreasing trend again. An opposite behaviour is shown by the

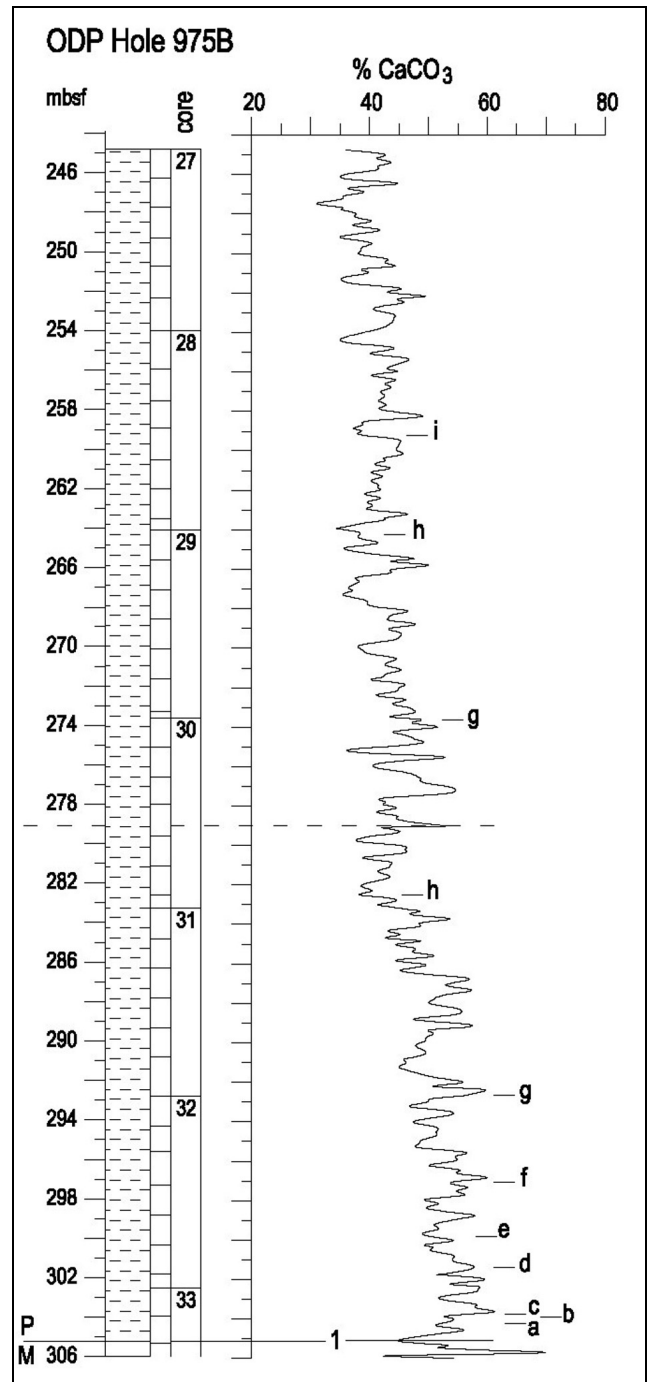


Fig. 7 - Curve of the calcium carbonate content and position of calcareous plankton events, as listed in Table 1. The dashed line indicates the point from which the supposed repetition of the section occurs.

*Calcidiscus* spp. group, that displays an increasing trend, followed by a sudden drop at ~279 mbsf. The “large” *Dictyococcites* spp. (>7 µm) category shows two high-abundance and two intervals lacking this group. Sphenoliths increase markedly in the uppermost part, where *G. rotula* and a lesser extent rhabdosphaerids and pontosphaerids also show increasing relative abundances (at the expense of *Dictyococcites* spp.). This may indicate an interval with improved preservation.

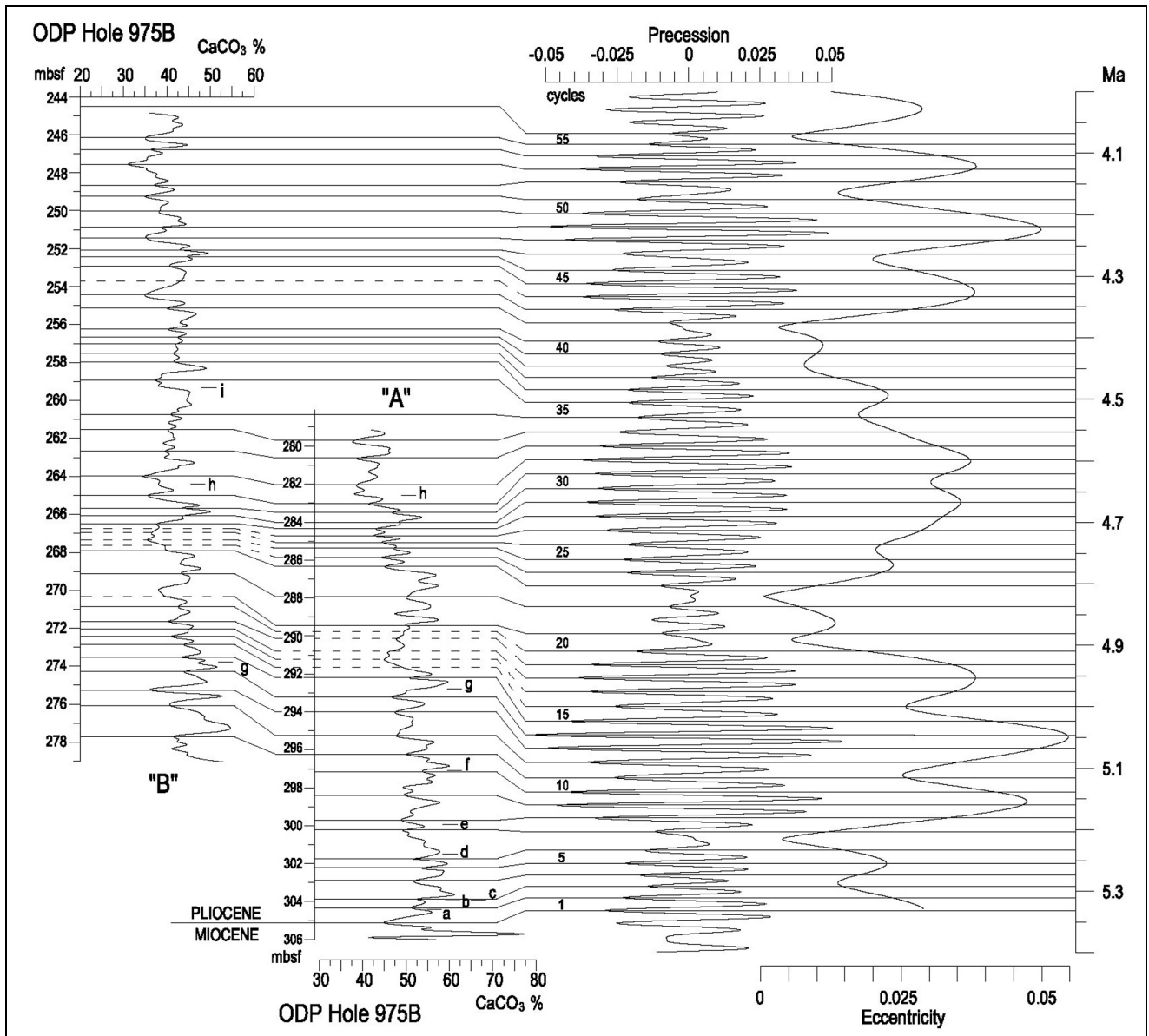


Fig. 8 - Curve of the carbonate contents subdivided into lower ("A") and upper ("B") tracts. Lower case letters indicate the biohorizons positions (Tab. 1). The numbers from 1 to 55 refer to the lithological cycles, coded after Lourens et al. 1996. The small-scale carbonate cycle patterns have been compared to precession and eccentricity data (Laskar et al. 2004). Dashed lines have been used when the lithological signal is less evident.

#### Data interpretation, cyclostratigraphic reconstruction and age model

The obtained data, expressed through abundance graphs, clearly high-light the presence of a break in the Hole 975B succession, at about 279 mbsf (dashed line in Fig. 5), marked by abrupt frequency variations of several nannofossil taxa. In some cases, similar trends seem to be repeated along the section.

Based on these patterns, the section has been separated into two tracts ("A" the lower and "B" the upper). The overlapping parts are shown in Fig. 6, which demonstrates how the curves of "large" and "small" *Dictyococcites* and *Calcidiscus* spp. display analogous trends within the overlapped intervals. The FCO

of *H. sellii* occurs at 264.35 mbsf, which seems to correspond to the beginning of the "anomalous presence" of this species recognized in the lower tract at 282.60 mbsf. Its stratigraphic distribution in Hole 975B makes better sense if part of the section is repeated. The partial overlap of the two tracts also explains the double paramere intervals of *R. pseudoumbilicus*.

The subsequent step of the study was to provide an accurate chronostratigraphic frame for the section in order to obtain more precise information about the repetition, than that offered by the graphic abundance patterns. Carbonate contents show distinct variations in the section (Fig. 7). These variations were interpreted from a cyclostratigraphic point of view, using the bios-

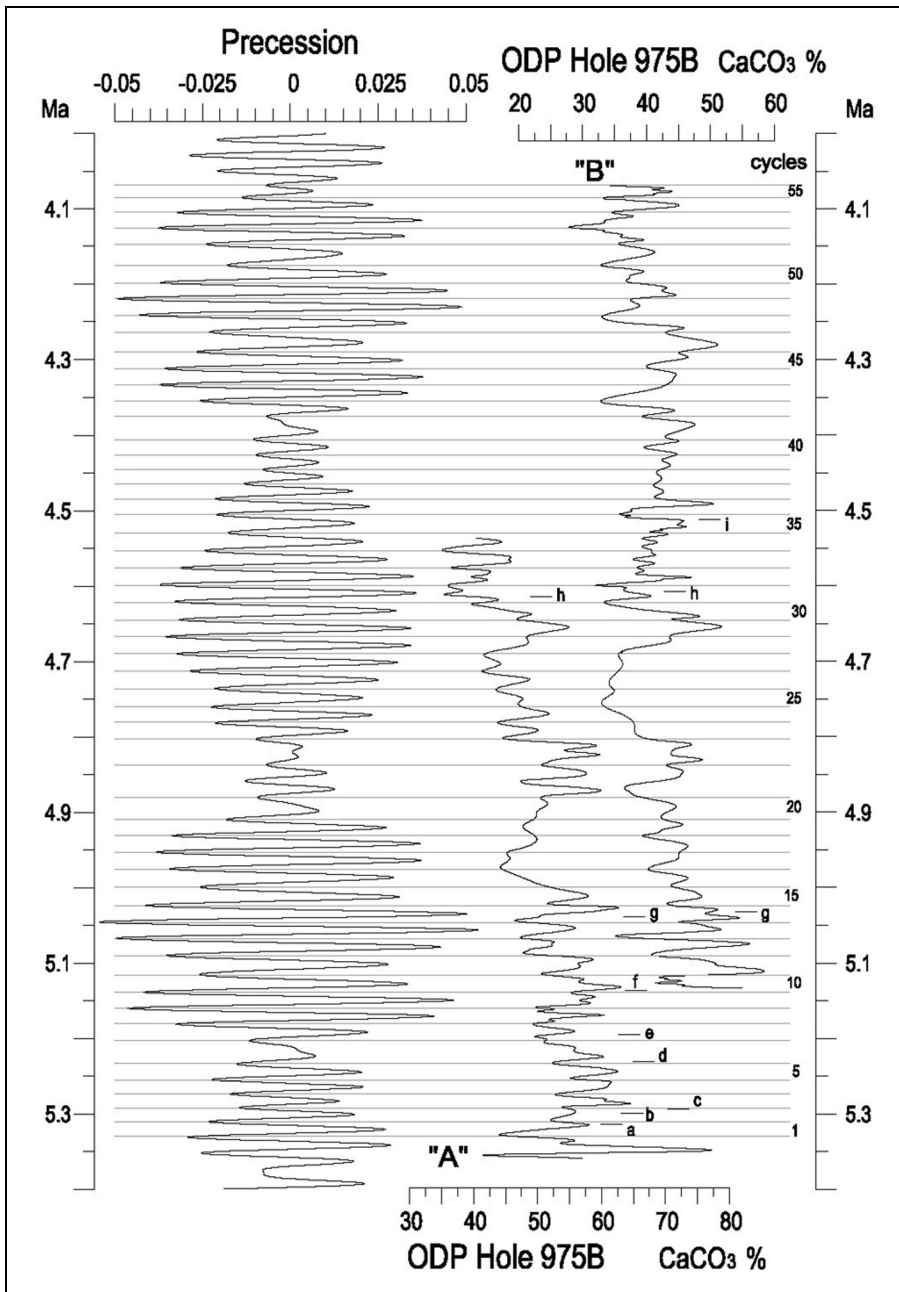


Fig. 9 - Age depth relationships obtained through plotting the  $\text{CaCO}_3$  variations vs age (Ma), and comparison of the small-scale carbonate cycle patterns with the precession (Laskar et al. 2004).

stratigraphic events listed in Tab. 1 as tie points. The position of the foraminifer events from “a” to “g” (Tab. 1) is after Iaccarino et al. (1999a, b). The position of the *Globorotalia puncticulata* FO (“i” in Tab. 1) at 259.35 mbsf, which slightly differs from that reported by Serrano et al. (1999), derives from an accurate revision of the planktonic foraminifer content, carried out by Dr. F. Riforgiato under the supervision of Prof. G. Salvadorini (University of Siena).

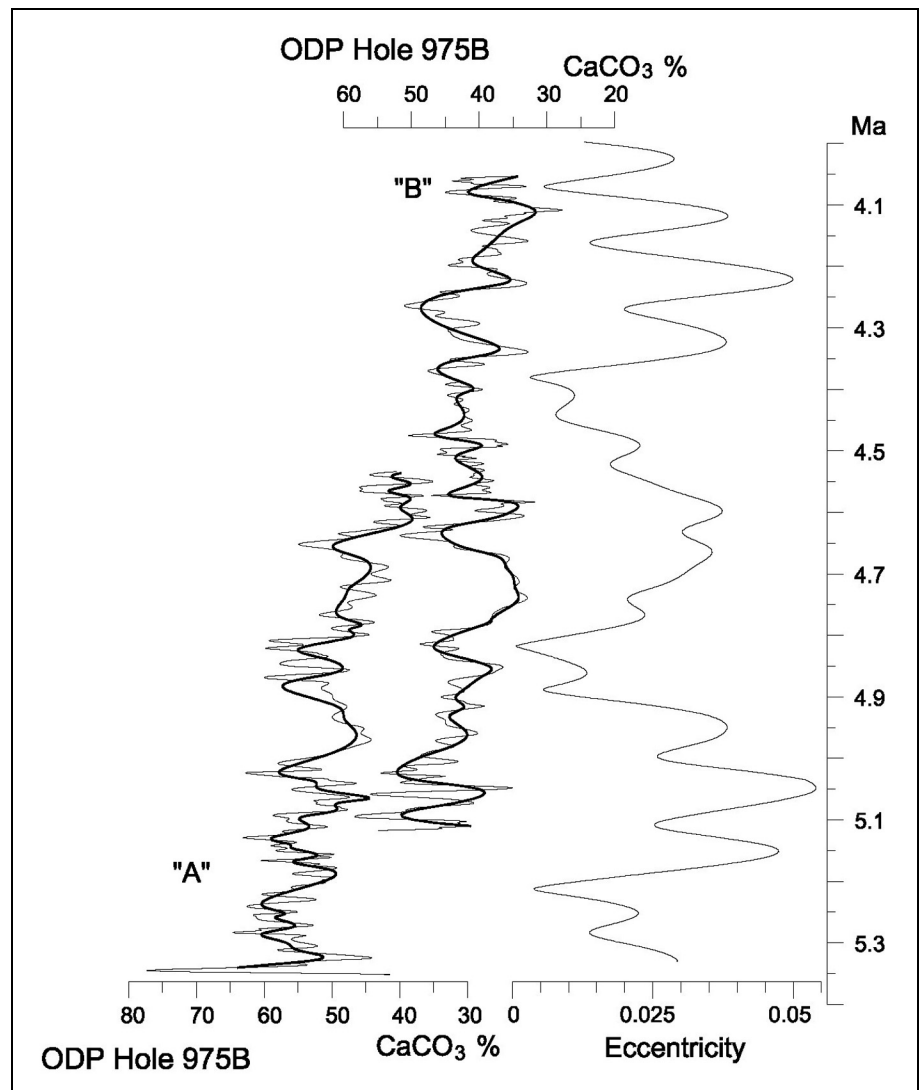
The carbonate curve was separated into the two tracts suggested by calcareous nannofossil abundance data. This curve hence has been subdivided into lithological cycles, coded after Lourens et al. (1996), and compared to changes in precession and eccentricity (Laskar et al. 2004) (Fig. 8). Changes in carbonate con-

tents of the basal tract (“A”) are well constrained by eight bioevents (Tab. 1), and can easily be correlated to the precessional variability.

The correlation between the two carbonate curve tracts is based on the positions of *R. pseudoumbilicus* Paracme End (PE) in cycle 14 (Di Stefano et al. 1999; Sgarrella et al. 1999; Di Stefano & Sturiale 2010) and *H. sellii* FCO in cycle 31 (Sgarrella et al. 1999; Di Stefano & Sturiale 2010). A further constrain is represented by the carbonate contents between 286.4 and 288.0 mbsf in the lower tract (“A”) and between 268.0 and 267.2 mbsf in the upper tract (“B”), which clearly corresponds to double cycle 22 of Lourens et al. (1996). The upper tract (“B”) is constrained by a unique bioevent, namely the FO of *G. puncticulata* in cycle 35 (Sprovieri 1993; Sgar-



Fig. 10 - Carbonate contents compared with eccentricity (Laskar et al. 2004). Note that higher percentages of  $\text{CaCO}_3$  are to the left. The bold line represents the tendency curve.



rella et al. 1999). The interval above cycle 35 lacks reliable biostratigraphic control. There, the lithological cycles corresponding to carbonate maxima have been correlated to the precession cycle closest to an eccentricity minimum, following Hilgen (1987; 1991).

According to this reconstruction, the basal tract ("A") of the section has been subdivided into 34 lithological (carbonate) cycles, starting from the M/Pb which marks the base of cycle 1. In the upper portion ("B") 45 cycles have been recognized, from cycle 11 to 55.

An age depth model is presented in Fig. 9. It is obtained from the correlation of the carbonate variations to the astronomically calibrated Pliocene cycles of Lourens et al. (1996). The final plotting of  $\text{CaCO}_3$  content vs. age was made using the AnalySeries program (Paillard et al. 1996). The good agreement with the precession curve is evident, except for some intervals where the precession signal is less clear, probably due to local disturbs originated by soft sediment sliding (Comas et al. 1996).

The carbonate curve has been re-plotted showing higher values to the left in order to emphasize its good

correspondence with eccentricity, even better highlighted by the tendency curve (Fig. 10).

These new data allowed re-calculation of the sedimentation rate along the two tracts of the section (Fig. 11). The diagrams have been obtained plotting the positions of the biostratigraphic events plus some additional tie points as listed in Tab. 1. The sedimentation rates within the lower ("A") and upper ("B") tracts shows near identical values.

The partial repetition of the succession is probably due to the presence of a huge slump fold. In fact, according to the description provided by Comas et al. (1996), similar structures affect other portions of the Hole 975B succession, e.g. in section 13H-4, between 113.5 and 114.5 mbsf.

## Conclusions

The Lower Pliocene interval of ODP Hole 975B is characterized by a sudden and unexpected increase of the sedimentation rate. This increase represents an arti-

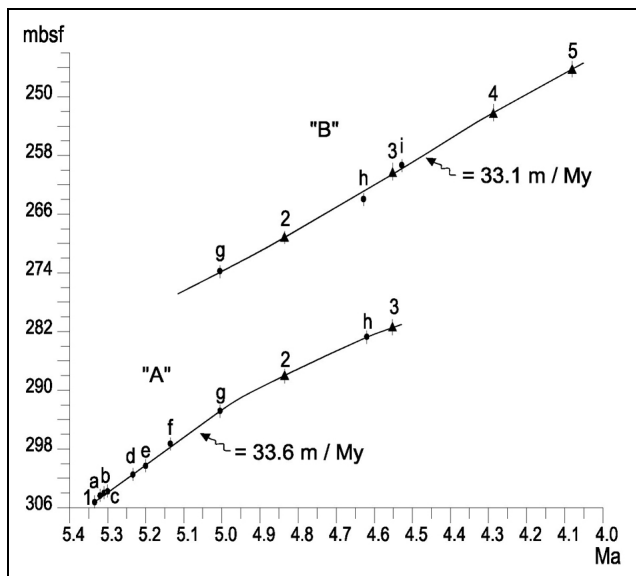


Fig. 11 - Sedimentation rates derived from positions of calcareous plankton bioevents and additional tie-points (Table 1) along the lower ("A") and upper ("B") tracts of the section versus age (Ma). Note similarity in sedimentation rates.

ficial repetition of the section, as demonstrated through a detailed stratigraphic study including quantitative biostratigraphy and cyclostratigraphy.

Based on these new data the succession has been subdivided into two tracts: the lower one is 26.22 m thick, spanning from the M/Pb at 305.22 mbsf to 279 mbsf, and covers a time interval of 0.780 Myr, corresponding to 34 lithological cycles, following the cyclostratigraphic code system of Lourens et al. (1996). This

lower tract begins from the base of cycle 1 at 5.332 Ma to the base of cycle 34 at 4.552 Ma. The upper tract is 34.2 m thick, spanning from 279 to 244.8 mbsf, and covers a time interval of 1.033 Myr, from cycle 11 at 5.115 Ma to cycle 55 at 4.082 Ma.

Thus, the 19.40 m thick tract between 298.4 and 279.0 mbsf, including cycles 11 to 34 (0.563 Myr), exactly corresponds to the stratigraphic interval between 279.0 and 259.6 mbsf.

Sedimentation rates, re-calculated using these new data, become very similar within the lower and the upper tracts, being 33.6 and 33.1 m/Myr, respectively.

This study demonstrates that accurate bio- and chronostratigraphic analyses help to explain anomalies in sedimentary successions as inferred presence of repetition (or gap) in absence of other macroscopic evidences. This may have relevance on wider geological aspects. As for the present study, the assertion that "...the lack of tectonic deformation and the paucity of slump structures..., suggest that Site 975 was tectonically inactive during Pliocene... time..." (pag. 142, Comas et al. 1996), should be revised.

*Acknowledgement.* I wish to thank Fabrizio Lirer, Simone Mineo, Giovanni Barreca and Gioconda Sturiale for their friendly help. Financial support is provided by "PRA University of Catania" grants (Responsible: Agata Di Stefano). Proff. Isabella Raffi and Jan Backman are warmly thanked for the care and patience in reviewing the original version of the manuscript.

This paper is dedicated to my father because I never dedicated something to him and because he deserves this and much more, in spite of his bad temper (too similar to mine).

## REFERENCES

- Cita M.B. (1975) - Studi sul Pliocene e gli strati di passaggio dal Miocene al Pliocene. VII. Planktonic foraminiferal biozonation of the Mediterranean Pliocene deep sea record: a revision. *Riv. It. Paleont. Strat.*, 81: 527-544.
- Comas M.C., Zahn R., Klaus A. et al. (1996) - Site 975. *Proc. ODP, Init. Repts.*, 161: 113-177.
- Di Stefano A. & Sturiale G. (2010) - Refinements of calcareous nannofossil biostratigraphy at the Miocene/Pliocene Boundary in the Mediterranean region. *Geobios*, 43:5-20.
- Di Stefano E., Cita M.B., Spezzaferri S. & Sprovieri R. (1999) - The Messinian-Zanclean Pissouri Section (Cyprus, Eastern Mediterranean). *Mem. Soc. Geol. Ital.*, 118: 133-144.
- Di Stefano E., Sprovieri R. & Scarantino S. (1996) - Chronology of biostratigraphic events at the base of the Pliocene. *Paleopelagos*, 6: 401-414.
- Fornaciari E., Di Stefano A., Rio D. & Negri A. (1996) - Middle Miocene quantitative calcareous nannofossil biostratigraphy in the Mediterranean region. *Micro-paleontology*, 42, 37-63.
- Hilgen F.J. (1987) - Sedimentary rhythms and high-resolution chronostratigraphic correlation in the Mediterranean Pliocene. *Newsl. Stratigr.*, 17: 109-127.
- Hilgen F.J. (1991) - Extension of the astronomically calibrated (polarity) time scale to the Miocene/Pliocene boundary. *Earth Planet. Sci. Lett.*, 104: 211-225.
- Iaccarino S., Castradori, D. Cita M.B., Di Stefano E., Gaborardi S., McKenzie J.A., Spezzaferri S. & Sprovieri R. (1999a) - The Miocene/Pliocene boundary and the significance of the earliest Pliocene flooding in the Mediterranean. *Mem. Soc. Geol. Ital.*, 54: 109-131.
- Iaccarino S.M., Cita M.B., Gaborardi S. & Gruppini G.M. (1999b) - High-resolution biostratigraphy at the Mio-

- cene/Pliocene Boundary in Holes 974b and 975b, Western Mediterranean. In: Zahn R., Comas M.C., Klaus A. (Eds) - *Proc. ODP, Sci. Res.*, 161: 197-221.
- Laskar J., Robutel P., Joutel F., Gastineau M., Correia A.C.M. & Levrard B. (2004) - A long term numerical solution for the insolation quantities of the Earth. *Astronomic Astrophysics*, 428: 261-285.
- Lourens L.J., Antonarakou A., Hilgen F.J., Van Hoof A.A.M., Vergnaud-Grazzini C. & Zachariasse W.J. (1996) - Evaluation of the Plio-Pleistocene astronomical timescale. *Paleoceanography*, 11: 391-413.
- Lourens L.J., Hilgen F.J., Laskar J., Shackleton N.J. & Wilson D. (2004) - The Neogene Period. In: Gradstein F. et al. (Eds) - *A Geological Time Scale*. Cambridge University Press: 409-440.
- Paillard D.L., Labeyrie L. & Yiou P. (1996) - Macintosh program performs time-series analysis. *Eos Trans, AGU* 77: 379.
- Rio D., Raffi I. & Villa G. (1990) - Pliocene-Pleistocene calcareous nannofossil distribution patterns in the Western Mediterranean. In: Kastens K.A. et al. (Eds) - *Proc. ODP, Sci. Res.*, 107: 513-533.
- Serrano F., González-Donoso J.M. & Linares D. (1999) - Biostratigraphy and paleoceanography of the Pliocene at Sites 975 (Menorca Rise) and 976 (Alboran Sea) from a quantitative analysis of the planktonic foraminiferal assemblages. In: Zahn R., Comas M.C., Klaus A. (Eds) - *Proc. ODP, Sci. Res.*, 161: 185-195.
- Sgarrella F., Sprovieri R., Di Stefano E., Caruso A., Sprovieri M. & Bonaduce G. (1999) - The Capo Rossello borehole (Agrigento, Sicily): cyclostratigraphic and paleoceanographic reconstructions from quantitative analyses of the Zanclean foraminiferal assemblages. *Riv. It. Paleont. Strat.*, 105, 2: 303-322.
- Sprovieri R. (1993) - Pliocene-early Pleistocene astronomically forced planktonic foraminifera abundance fluctuations and chronology of Mediterranean calcareous plankton bio-events. *Riv. It. Paleont. Strat.*, 99: 71-414.
- Sturiale G. (2008) - Calcareous nannofossil quantitative analysis of selected Neogene intervals: biostratigraphic, paleoclimatic and paleoceanographic considerations. Unpubl. doctoral dissertation, Dept. of Geological Science, University of Catania, XXI cycle: 203 pp.

